

## Multiple Stimulated Raman Scattering in Glass Optical Fibers

FELIPE RUDGE BARBOSA and RAMAKANT SRIVASTAVA

*Instituto de Física "Gleb Wataghin", UNICAMP, Campinas, SP*

Recebido em 21 de Outubro de 1981

Due to their extremely large interaction lengths, optical fibers can be very convenient for observation of non-linear optical phenomena. In this work we present an extensive study of Stimulated Raman Scattering (SRS) in fibers with different characteristics. Our observations include spectra, measurements of thresholds and of power conversion from pump to multiple Stokes radiation. As many as eleven Stokes orders have been observed in a singlemode fiber, and up to seven Stokes and four anti-Stokes orders in a quasi-singlemode fiber. Our results on power conversion show that even in the case of near total pump depletion, pump power and fiber length are equivalent parameters for SRS, although this equivalence cannot be fully understood on the basis of existing theoretical models.

Devido aos comprimentos de interação extremamente longos conseguidos em fibras ópticas, estas podem ser muito convenientes para observação de fenômenos não-lineares. Neste trabalho apresentamos um estudo extensivo do espalhamento Raman estimulado (SRS) em fibras com diferentes características. Nossas observações incluem espectros, medidas de limiares e medidas de conversão de potência da radiação de bombeio (laser) para múltiplas linhas Stokes. Até 11 ordens Stokes foram observadas numa fibra monomodo, e até 7 ordens Stokes e 4 anti-Stokes numa fibra quasimonomodo. Nossos resultados de conversão de potência mostram que, mesmo no caso de depleção quase total do bombeio, a potência de bombeio e o comprimento da fibra podem ser parâmetros equivalentes para o SRS, apesar de que esta equivalência não possa ser bem entendida com base nos modelos teóricos existentes.

## 1. INTRODUCTION

In optical communication systems, fibers are presupposed to be linear elements. However, it has been recognized for some time that optical fibers in general<sup>1-3</sup>, and glass optical fibers in particular<sup>4</sup>, may show marked non-linear behavior at moderate input powers, because once light is coupled into the fibre core it is maintained there at high power densities and long interaction lengths. For inputs of less than 100 W (small if compared with non-linear optics standards) a fiber is capable of generating, mixing and recombining frequencies to such extent that output may radically differ from input. Among reported effects are stimulated Raman<sup>5</sup> (SRS) and Brillouin scattering<sup>6</sup> (SBS), three-<sup>7</sup> and four-wave<sup>8</sup> mixing, and self-phase modulation<sup>9</sup>. For broadband signals (> 10GHz) only SRS will prevail provided that pump powers are strong enough for the Raman gain<sup>10</sup> to be able to exceed losses and yield amplification of Raman light. Several fiber Raman amplifiers and oscillators have been reported over the last decade<sup>1,3-5</sup>, but in spite of the vigorous efforts in the study of non-linear phenomena in fibers, there are some gaps on both experimental and theoretical grounds that still need to be filled. In particular, the study of stimulated Raman effect has been lacking a consistent and comprehensive work regarding the dependence of the various parameters (such as pump wavelength, pump power, fibre length, core diameter, etc.) under the same basic experimental conditions - for only in this case a comparative study is meaningful, and in practice useful. It is this gap that the present work intends to fill.

Using the same excitation (laser) and detection system, and varying the samples only, we have obtained spectra and measured the thresholds of several Stokes and anti-Stokes orders of SRS as a function of fiber length, core diameter and pump frequency; also included are measurements of frequencies and pump to Raman energy conversion in multiple stimulated Stokes and anti-Stokes generation as a function of pump power and fiber length. We have observed in a singlemode fiber as many as 11 distinct Stokes orders, absence of anti-Stokes SRS and total laser depletion. We demonstrate that in a fiber, pump power and sample length can be equivalent parameters even in the regime of near

total pump depletion. In section 2 a brief account of existing theoretical bases of SRS is presented, the particular case of fibers is considered, and although the present work is essentially experimental this section is included for completeness, so that the reader does have to refer necessarily to the original works on theory. Discussion of our observations in section 3 shows that existing models based on various pump beam profiles and geometrical configurations do not adequately describe our data.

## 2. THEORY

Stimulated Raman scattering is a coherent non-linear effect that comes from the direct coupling of the Stokes optical field to the laser field through the third order term in the power expansion of the polarization<sup>11</sup>:

$$\vec{P}_{NL}^{(3)}(\vec{x}, t) = \chi^{(3)}(\vec{x}, t) : \vec{E}_L(\vec{x}, t) \vec{E}_L^*(\vec{x}, t) \vec{E}_S(\vec{x}, t) ,$$

where  $\chi^{(3)}$ , the coupling parameter, is the third order non-linear susceptibility, a tensor of 4th rank;  $\vec{E}_L(\vec{x}, t)$  and  $\vec{E}_S(\vec{x}, t)$  are the Laser and Stokes optical fields. Since glass has inversion symmetry this is the only non-linear polarization prevailing; in fibers, due to the co-linear confinement of radiation, the vector notation can be dropped and  $\chi^{(3)}$  taken as a scalar. For the theoretical treatment of SRS it is convenient to express the non-linear polarization in terms of its frequency components<sup>11</sup>; for Stokes frequencies

$$P_{NL}^{(3)}(\omega_s) = \chi^{(3)}(-\omega_s; \omega_L, -\omega_L, \omega_s) E_L(\omega_L) E_L^*(\omega_L) E_S(\omega_s) ,$$

where the energy conservation condition  $\omega_s = \omega_L - \omega_L + \omega_s$  is implied in the  $\chi^{(3)}$  argument. In this case, phasematching conditions  $\pm \vec{k}_s = \vec{k}_L - \vec{k}_L \pm \vec{k}_s$  (forward (+) and backward (-) Stokes waves) are readily fulfilled, and stimulated Stokes light is said to be self-phase matched. For anti-Stokes (AS) radiation the situation is somewhat more involved<sup>11</sup> since

$$P_{NL}^{(3)}(\omega_{AS}) = \chi^{(3)}(-\omega_{AS}; \omega_L, \omega_L, -\omega_S) E_L(\omega_L) E_L(\omega_L) E_S^*(\omega_S) ,$$

requires that Stokes light be present so that  $\omega_{AS} = \omega_L + (\omega_L - \omega_S)$  holds. Physically, the presence of stimulated Stokes lights inverts the vibrational population of the medium, and the laser light induces this population to normal distribution, yielding in the process the stimulated AS light. Phase-matching  $\pm \vec{k}_{AS} = 2\vec{k}_L \pm k_S$  (forward (+-), backward (-+)) is not readily fulfilled. Actually, in a rigorous singlemode fiber, this condition is never fulfilled<sup>12</sup>, therefore stimulated AS radiation will not appear in such a fiber. This aspect will be further discussed in Sect. 3.b.

Stimulated Stokes light is generated by the build up of spontaneous Raman scattering, which takes place through the coupling of the incident laser light and the vibrational modes of the medium. For small pump intensities it varies linearly with sample length<sup>3</sup>

$$I_R = \sigma_R I_L(z) z , \quad (a)$$

$\sigma_R$  is the Raman cross-section,  $I_R$  and  $I_L$  are the Raman and laser intensities. The above expression remains valid as long as pump is not depleted in the process, with attenuation along sample length given by  $I_L = I_L(0) e^{-\alpha z}$  (Beer's law), where  $\alpha$  represents all losses per unit length. If the pump intensity is increased, the Raman scattered intensity increases linearly until losses are equaled by Raman gain, and threshold for SRS is achieved; whichever Stokes line, or band, has largest gain will prevail upon other vibrations and grow very rapidly becoming comparable to the pump intensity. In this stimulated regime, the rate equation for  $I_R$  and  $I_L$  must allow for the gain,

$$\frac{dI_R}{dz} = g I_R I_L - \alpha I_R , \quad (b)$$

with the Raman gain  $g$  at the Stokes frequency given by<sup>10</sup>

$$g = \frac{\sigma \lambda_s^3}{c^2 h \epsilon(n+1)}$$

where,  $a$  is the Raman differential cross-section,  $\lambda_s$  the Stokes wavelength,  $\epsilon$  the dielectric constant at the Stokes frequency and  $n$  the Bose-Einstein population factor;  $c$  and  $\hbar$  are velocity of light in the medium and Planck's constant, respectively. In equation (b), negligible spontaneous emission into Stokes mode is assumed. At the threshold of SRS the depletion of pump photons is small and may be neglected, so we have again  $I_L = I_L(0) e^{-\alpha z}$ . Thus, integrating (b) we have

$$I_R(z) = I_R(0) \exp \left\{ g \left[ \frac{1 - e^{-\alpha z}}{\alpha} \right] I_L(0) - \alpha z \right\}, \quad (c)$$

which reveals the fast growth of SRS due to its exponential dependence on pump intensity.  $I_R(0)$  represents the spontaneous scattering as the input end of fiber. Finally, if the pump intensity is increased well beyond the threshold of the first stimulated Stokes order, a marked energy conversion of pump to Stokes photons takes place and higher order stimulated Raman radiation appears both on the Stokes and anti-Stokes lines are not generated. In this regime (well above threshold) each Stokes order is intense enough to serve as pump to the next, and the rate equation for  $I_R$  and  $I_L$  is no longer one but a system of several coupled equations, in which pump depletion is taken into account<sup>13,14</sup>. The rate equations can be written as:

$$\frac{dI_L}{dz} = -g_L I_L I_{S1} - \alpha_L I_L$$

$$\frac{dI_{S1}}{dz} = +g_{S1} I_L I_{S1} - \alpha_{S1} I_{S1} - g_{S2} I_{S1} I_{S2}$$

$$\frac{dI_{S2}}{dz} = +g_{S2} I_{S1} I_{S2} - \alpha_{S2} I_{S2} - g_{S3} I_{S2} I_{S3},$$

and so on;

the  $I_{S_i}$  stand for Stokes orders, the  $\alpha_{S_i}$  for the losses at the corresponding frequencies and the  $g_{S_i}$  for the frequency dependent gain coefficients.

Such system has been solved for four Stokes orders, assuming plane wave profile for the laser light<sup>13</sup>, and later modified to the

gaussian (fundamental) laser beam profile<sup>14</sup>. These cases are reproduced in Figure 1a and b, respectively; both yield pump depletion and multiple SRS generation, as well as a saturation effect that prevents each Stokes line from growing indefinitely. This happens because as the growing intensity of a Stokes line reaches the threshold of the next a

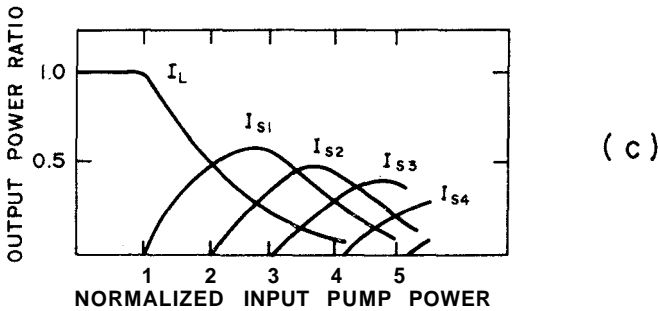
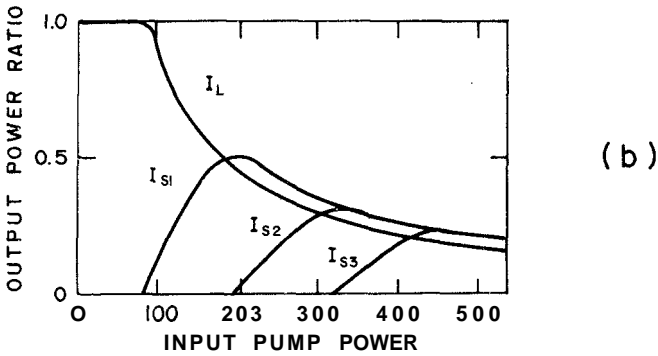
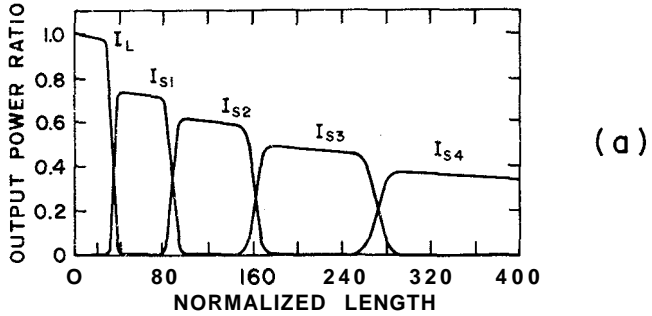


Fig.1 - Laser to Stokes SRS power conversion: a) dependence with sample length assuming plane-wave pump profile (after ref.17); b) dependence with pump intensity for gaussian pump profile (after ref. 18); c) dependence with pump intensity for a multimode liquid-core fiber (after ref. 21).

flow of power sets in depleting that line. The theoretical predictions of the gaussian case have been confirmed experimentally in a liquid cell geometry<sup>14</sup>, whereas no experiments have been performed to this date for the plane-wave case. To conclude this part we mention that a recent model proposed for SRS in fibers<sup>15</sup>, is not a satisfactory as the two above and does not account for multiple SRS generation. Moreover, existing experimental evidence<sup>16</sup> of pump to Raman power conversion in a multimode liquid core fiber does not fit any model properly.

### 3. EXPERIMENTAL & DISCUSSION

#### A. Experiiments and Results

The experimental configuration shown in Figure 2 is standard. Laser power from a pulsed dye-laser excited by lamp, operating in the 590-620 nm range with a  $3 \text{ cm}^{-1}$  linewidth and  $1 \mu\text{s}$  pulse width, is focused with a  $20\times/0,40$  microscope objective into fiber core. Fiber output is collected with a photographic objective chosen to match the spectrometer optics and, either focused into a double spectrometer, detected

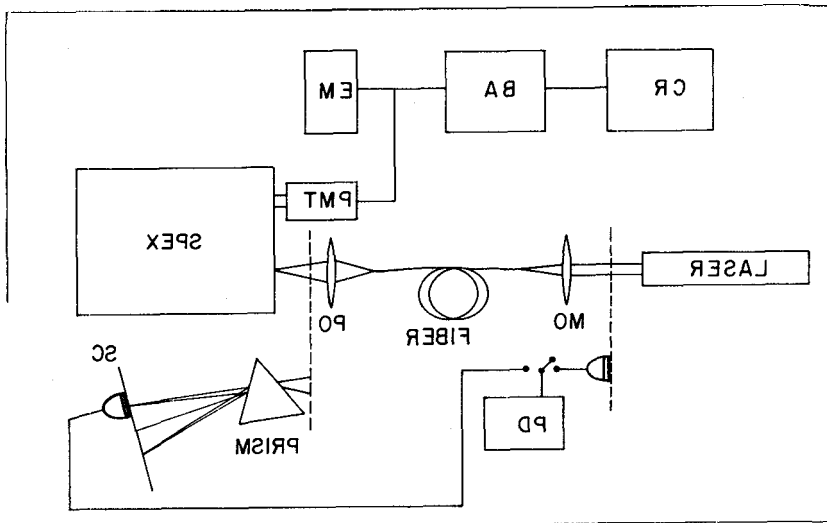


Fig.2 - Schematics of experimental arrangement. MO and PO are objectives. PD is photodetector. EM, BA and CR are electrometer, box-car amplifier and recorder, respectively.

in a photomultiplier and averaged in a box car amplifier, or dispersed with a flint prism onto a screen for visual observations and photography. Fibers used has a Ge doped SiO<sub>2</sub> core diameters of 5μm, (W-index profile), 8μm and 15μm (step-index profile) - henceforth Fiber 5, Fiber 8 and Fiber 15 - supplied by Valtec Corp. (USA), Bell Labs. (USA) and CPqD - TELEBRÁS (Brasil), respectively. These fibers were cut and used in lengths ranging from 15m to 500m (no splices). Overall coupling of laser to fiber varied to different fibers, but was reproducible with optimal values as follows: 55% for Fiber 5, 70% for Fiber 8 and 80% for Fiber 15. Below we present the bulk of our experimental observations.

*Thresholds* (Table 1): The smaller the core diameter the lower the threshold for Stokes and anti-Stokes SRS, because very high intensities inside the fiber may be achieved with moderate powers of the pump beam (e.g., few tens of watts of pump will lead to several tens of MW/cm<sup>2</sup> inside the fiber). Increasing pump wavelength lowers threshold for SRS within our working range (590-620 nm).

TABLE 1: Thresholds for the various SRS orders in fibers. (Arbitrary units, see note on Fig.5). Dots mean not measured, dashes mean in-existent.

Fiber Length	Laser Wavelength	2 <sup>o</sup> AS	1 <sup>o</sup> AS	1 <sup>o</sup> S	2 <sup>o</sup> S	3 <sup>o</sup> S	4 <sup>o</sup> S
Fiber 5	600 nm	-	-	1,1	2,8	3,3	...
<i>L</i> = 30 m	610 nm	-	-	0,2	1,2	2,2	2,6
Fiber 5	600 nm	-	-	0,4	1,3	2,9	4,7
<i>L</i> = 400m	610 nm	-	-	0,2	0,7	1,7	2,5
Fiber 8	600 nm	4,6	3,7	2,8	3,7	4,4	...
<i>L</i> = 30 m	610 nm	...	2,5	1,7	2,3	3,1	...
Fiber 15	600 nm	...	8,8	4,4	9,0	12,0	...
<i>L</i> = 30 m	610 nm	...	5,8	3,1	6,3	9,2	10,2



*Stokes* (Table 2, Figures 3 and 4): All fibers in length ranging from 15m to 500m show a profusion of stimulated Stokes radiation. Up to 11 orders of Stokes light were recorded (Fig.3) for 100m of Fiber 5 (extending from visible 610nm to near infrared 870 nm); for 30 m of Fiber we recorded (Fig. 4) 6 Stokes orders; and for 270m of Fiber 15 we observed up to 8 Stokes orders. The separation between successive orders was of  $440 \text{ cm}^{-1}$  (the main Raman shift of silica) with a typical deviation of  $\pm 20 \text{ cm}^{-1}$ , as can be seen in Table 2. This is verified, as expected, for various pump wavelengths from 595 to 615nm.

*Anti-Stokes* (Table 2, Figure 4): In 30m of Fiber 15 we could observe only two orders of anti-Stokes SRS radiation, because intensities inside the fiber are smaller for a large core. For the same length of Fiber 8, four orders of anti-Stokes SRS are distinctly observed (Figure 4). On the other hand, for Fiber 5 anti-Stokes SRS was not observed, no matter how much power or length of fiber was used. Contrary to Stokes lines, the frequency separation for anti-Stokes is not the same for different fibers, within the  $\pm 20 \text{ cm}^{-1}$  allowance; Fiber 15 has the expected  $440 \text{ cm}^{-1}$  separation between successive lines; Fiber 8, however, shows a peculiar feature of  $400 \text{ cm}^{-1}$  separation between some lines and  $500 \text{ cm}^{-1}$  between the second and third lines (Table 2).

*Conversion* (Figure 5): Depletion of laser photons is always observed for intensities above the first Stokes order threshold, and the longer the fiber the higher the conversion; for 500m of fiber 5 we obtain a "total" conversion of 100% (actually the output at laser frequency is less than 0,1%), whereas for 15m of the same fiber the observed conversion is less than 50%. For a given length of fiber we observe increased conversion for increasing pump intensity and saturation effect of various Stokes orders.

Stimulated backward scattering has been observed in all fibers and lengths. Measured thresholds are higher than corresponding forward threshold. All other parameters show the same behavior as forward SRS.

Table 2: Absolute frequencies in  $\text{cm}^{-1}$  of laser and the various SRS orders in fibers.

Fiber 5 (100 m)	Laser	1 $\text{st}$ S	2 $\text{nd}$ S	3 $\text{rd}$ S	4 $\text{th}$ S	5 $\text{th}$ S	6 $\text{th}$ S	7 $\text{th}$ S	8 $\text{th}$ S	9 $\text{th}$ S	10 $\text{th}$ S	11 $\text{th}$ S
	16600	16150	16680	15320	14790	14360	13930	13470	13040	12620	12190	11750
Fiber 8 (30 m)	4 $\text{th}$ AS	3 $\text{rd}$ AS	2 $\text{nd}$ AS	1 $\text{st}$ AS	Laser	1 $\text{st}$ S	2 $\text{nd}$ S	3 $\text{rd}$ S	4 $\text{th}$ S	5 $\text{th}$ S	6 $\text{th}$ S	7 $\text{th}$ S
	18300	17900	17400	17000	16600	16160	15720	15270	14830	14400	13950	13500
Fiber 15 (240 m)	2 $\text{nd}$ AS	1 $\text{st}$ AS	Laser	1 $\text{st}$ S	2 $\text{nd}$ S	3 $\text{rd}$ S	4 $\text{th}$ S	5 $\text{th}$ S	6 $\text{th}$ S	7 $\text{th}$ S	8 $\text{th}$ S	.....
	17480	17040	16600	16150	15700	15250	14820	14400	13970	13600	13200	.....

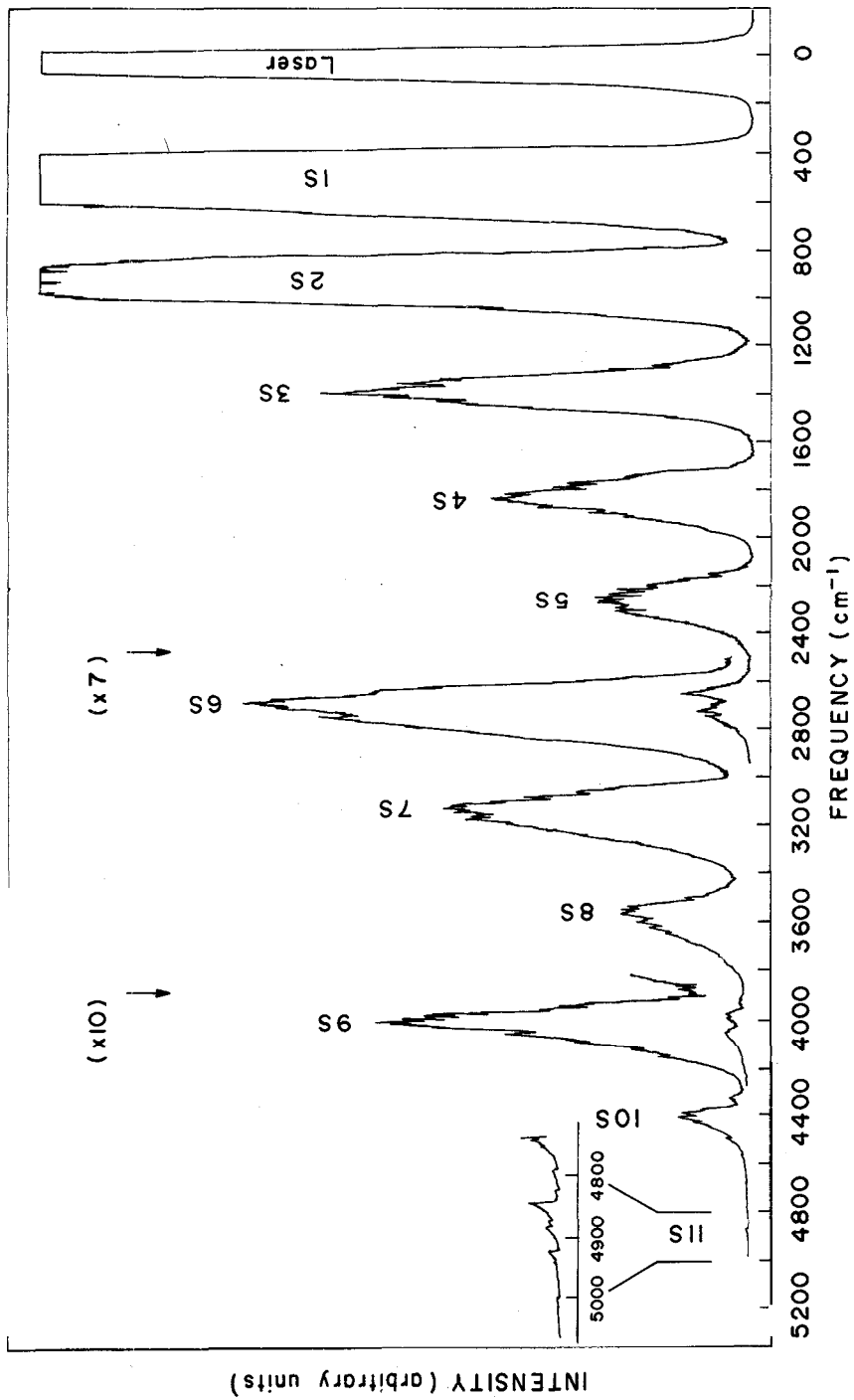


Fig. 3 - Spectrum of multiple Stokes SRS from 100m of Fiber 5.

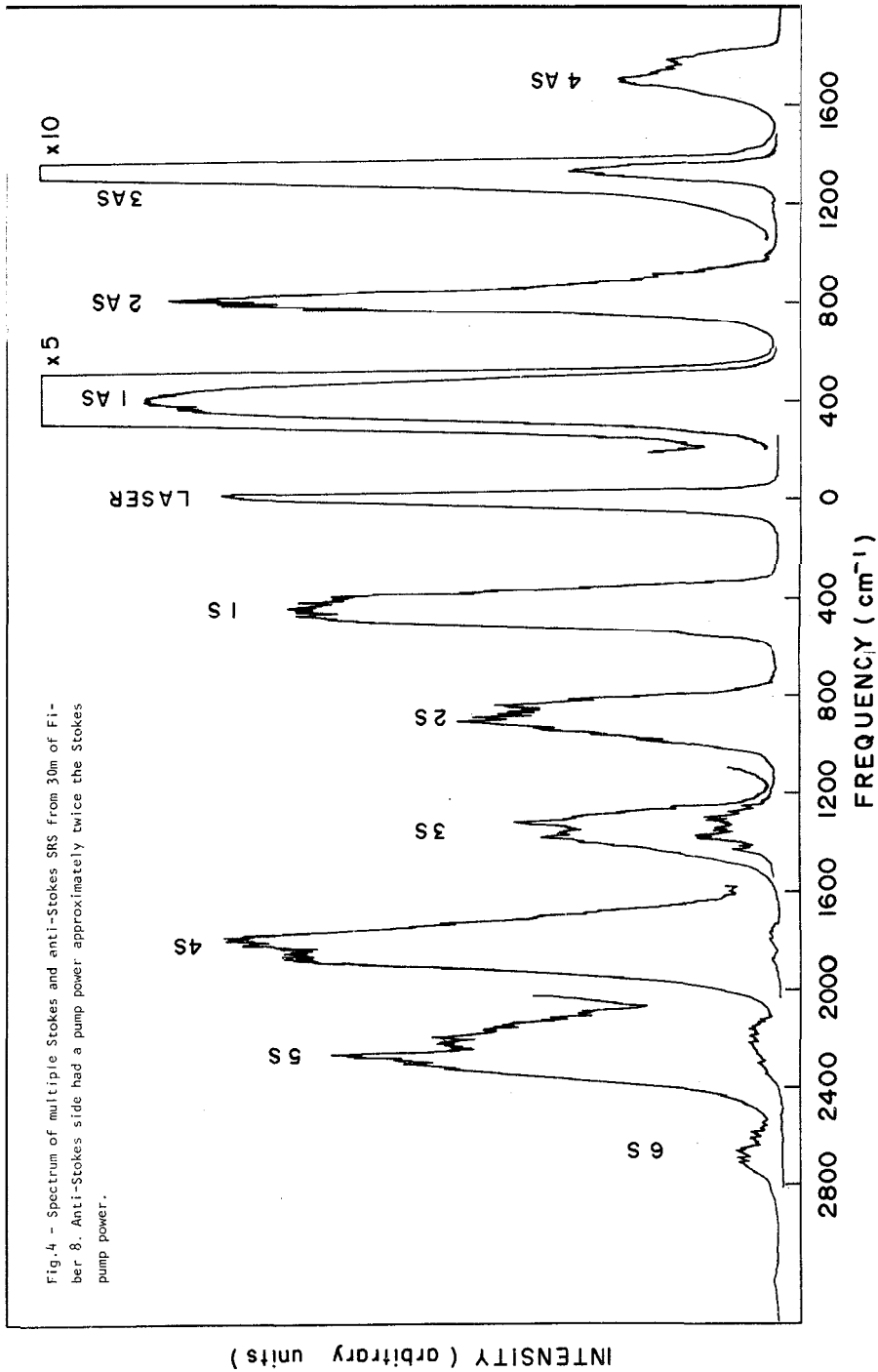


Fig.4 - Spectrum of multiple Stokes and anti-Stokes SRS From 30m of Fiber 8. Anti-Stokes side had a pump power approximately twice the Stokes pump power.

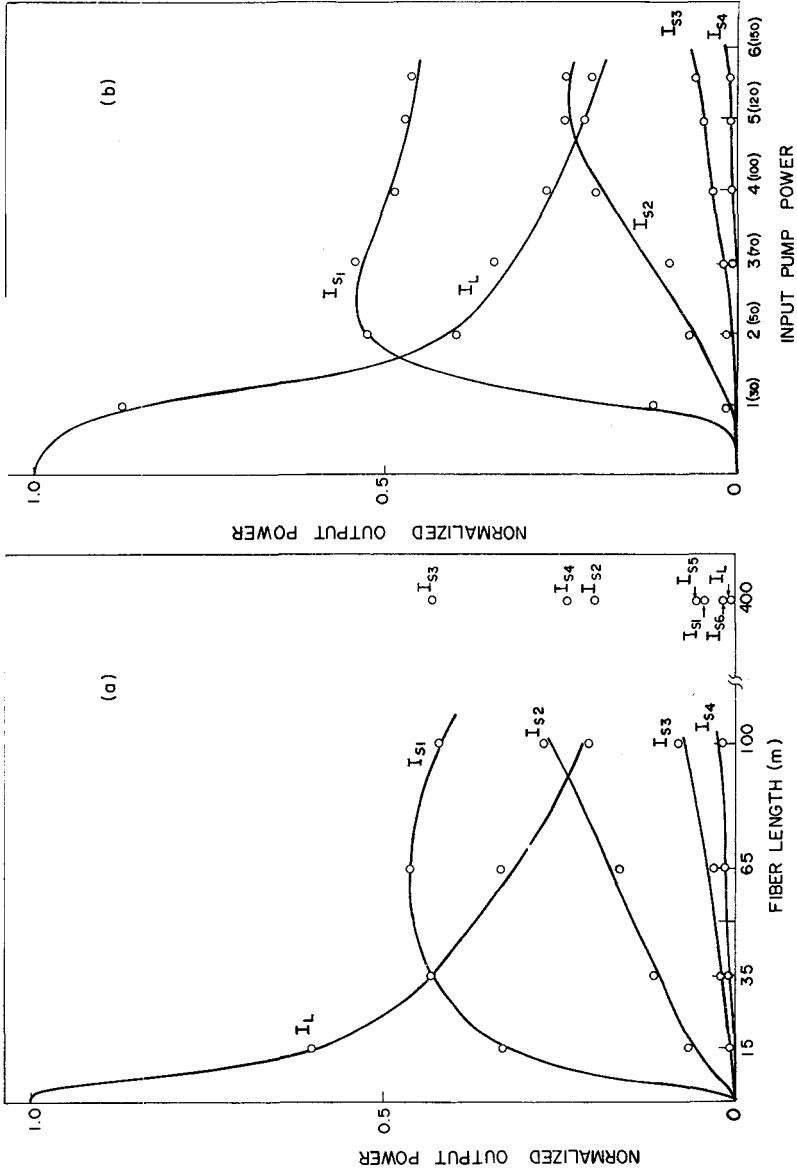


Fig. 5 - Measured laser to Stokes SRS power conversion: a) dependence with fiber length (Fiber 5) and b) dependence with pump power (Fiber 5, 65m). Note: values in parenthesis on the input power axis are the approximate equivalent in watts, with an error of  $\pm 5\%$ , of the average pulse peak power.

## B. Discussion

Observations concerning thresholds are self-explanatory and need no further discussion; however, we should add some comments. At longer pump wavelengths thresholds are smaller because fibers exhibit less attenuation at these frequencies. In other words, lower input powers will still maintain the high intensities required for efficient SRS generation. This, however, is not true in the infrared where some strong absorption bands occur. The observations of backward SRS are consistent with theoretical predictions and results are basically the same as for forward SRS, with the exception of higher thresholds, therefore we decided to discontinue the study of backward SRS.

Conversion of laser light to higher order Stokes and anti-Stokes SRS, i.e., multiple SRS generation, is the main concern of the present work. It can be obtained either by increasing pump power keeping fiber length fixed, or by increasing fiber length and keeping input pump power fixed. We have observed that the two can be equivalent. Ippen<sup>16</sup> has studied the former case in a multimode liquid core fiber filled with CS<sub>2</sub> and we have studied both in a singlemode solid core fiber. Figure 1c shows Ippen's results for dependence of pump power conversion with input pump intensity and Figure 5 shows our results for the dependence of pump power conversion with (a) fiber length, and (b) input pump intensity; equivalence is clear. These curves bear a remarkable resemblance with those obtained by Ippen (Fig.1a) in the multimode liquid-core fiber. However, several comments pertain here. Our results should, in principle, agree with the previous gaussian beam profile results (Fig.1b), and disagree with the multimode fiber results (Fig.1c), because the intensity profile of a singlemode fiber is gaussian (Figure 6), even if the pump beam is not, as was our case. Since in a multimode fiber, higher order Stokes do not necessarily propagate in the same mode as the pump does, one would expect smaller overlap between the fields and thereby a different behavior for pump to Stokes conversion. On the other hand, it has been suggested<sup>16</sup> that a singlemode fiber should yield results similar to the plane-wave case (Fig. 1a), but our results (Fig.5) do not confirm this. Furthermore, the multiple SRS radiation in our singlemode fiber differs appreciably from previous work<sup>14</sup> using a liquid CS<sub>2</sub> cell, where gaussian beam profile

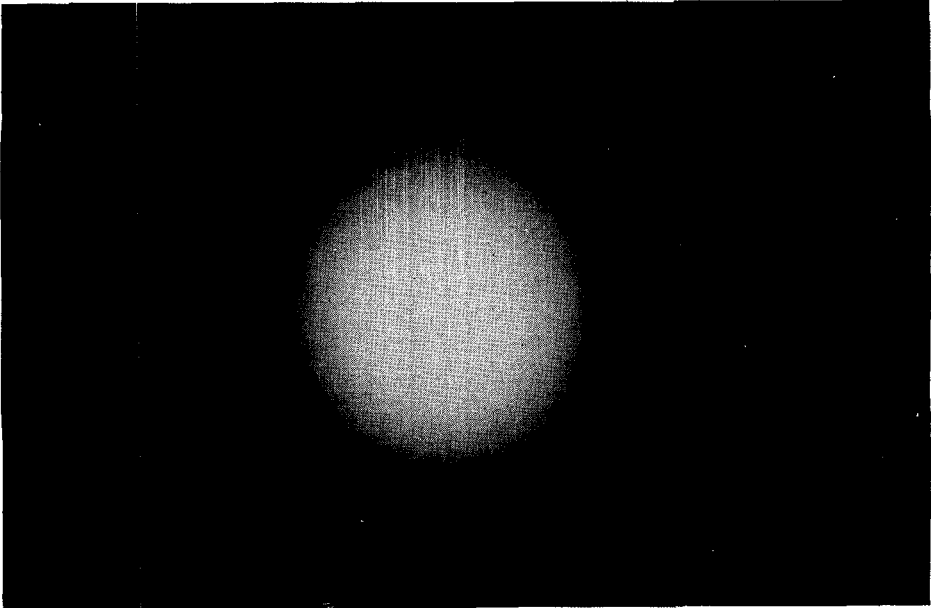


Fig.6 - Gaussian profile output of Fiber 5.

calculations were confirmed experimentally. Before we try to elucidate these discrepancies, let us make some further considerations. From Fig. 5, and Fig. 1a 6 b we see that laser and Stokes intensities fall off much faster in fig. 5 than in the gaussian case and more slowly than in the plane-wave case; the latter discrepancy is easily explained as follows: when the laser intensity is depleted to below the first Stokes threshold it becomes uncoupled to the Stokes optical field and then is attenuated only by the losses in the medium, which are much less severe than the nonlinear effect; this mechanism is not taken into account in any model. The fact that the laser intensity in fibers falls off more rapidly than that predicted by the gaussian model<sup>14</sup> appears to be caused by a confinement of pump power over much longer distances in fibers as compared to a liquid cell, causing thereby its depletion by the stimulated Raman process.

Of greater difficulty would be a detailed theoretical description of the behavior of the various Stokes orders in Fig. 5a and 5b. The curves of Fig. 5a indicate that different lengths of fiber lead to different conversion efficiencies for the same input power; actually,

in a long fiber (400 m), we have observed that the transmitted laser intensity is at most equal to the first Stokes intensity, and as power is increased higher Stokes orders reach intensities well-above those of the first Stokes and transmitted laser lines. From Fig. 5a we can also see that each higher order Stokes line is generated, or better, attains a maximum inside the fiber, further from the input end. In addition, as fiber length increases thresholds decrease and conversion of power to higher orders increases.

These observations indicate that the complex nonlinear behavior of a fiber, especially if long, is due to the unusual property that fibers have of maintaining light confined at very high intensities (hundreds of MW/cm<sup>2</sup>) over its whole length - thereby yielding results that cannot be predicted using other geometries. The fact that a single-mode glass fiber with small Raman gain (as ours), and a multimode liquid-core fiber<sup>16</sup> with high Raman gain, unexpectedly show the same behavior, tends to confirm the above statement. Presently we are developing a theoretical description that will include the light confinement at high intensities along the fiber core; this will modify existing models and contribute to a better understanding of SRS in fibers.

Finally we discuss the stimulated anti-Stokes scattering. In the case of multimode fibers it is generated by the third-order parametric coupling of stimulated Stokes and pump fields<sup>12</sup>. Phase-matching (k-vector conservation) is in general very critical for parametric processes, and for isotropic materials it cannot be satisfied for collinear interaction due to normal material dispersion. In fibers, however, the multimode structure of the waveguide (depicted in Fig.7) allows light of different frequencies to propagate in different modes of different k-vectors, that are able to fulfill the conditions  $\vec{k}_{AS} = 2\vec{k}_L - \vec{k}_S$  of linear momentum conservation. This is the case of Fiber 15 which, according to Ref. 17 (see Appendix) has  $V = 8.6$  at 600 nm pump frequency and approximately 36 propagating modes; Fiber 15 can satisfy very easily the  $\vec{k}$ -conservation condition and yield stimulated AS scattering at multiple integers of the main Raman shift (440 cm<sup>-1</sup>), as can be seen in Table 2. The extreme opposite case is Fiber 5, which has  $V \approx 2.1$  at 600nm, and exactly two degenerate modes of propagation (which have the same b value in Fig.7); the two modes are occupied by



$\vec{k}_L$  (laser) and  $\vec{k}_S$  (Stokes), and the parametric coupling condition cannot be satisfied because there are no other propagation modes available. In this case stimulated AS radiation does not appear, as seen in Table 2 and Fig. 3. At last, the intermediate case of a fiber with a few propagating modes will be considered. Fiber 8 has  $V=4.2$  at 600 nm with less than 10 propagating modes; this means that enough modes are available in order to satisfy phase-matching. Since only a few modes can propagate it is possible that stimulated AS multiple integer shifts  $\Delta\bar{\nu}_{AS} = n\Delta\bar{\nu}_0$ ,  $\Delta\bar{\nu}_0 = 440 \text{ cm}^{-1}$ , do not coincide with allowed phase-matched propagation frequencies. We verify that this possibility is realized in practice, as shown in Fig. 4 and Table 2. We explain these "odd" shifts as a self-accomodation mechanism where the anti-Stokes Raman gain is no longer centered at the main silica shift<sup>18</sup> but moves to a convenient frequency  $\vec{k}_S$  in order to satisfy phase-matching. Energy conservation will be, of course, still maintained because observed shifts fall within the stimulated linewidths, but AS lines are consequently narrowed since maximum intensities are not matched, as can be seen in Fig. 4.

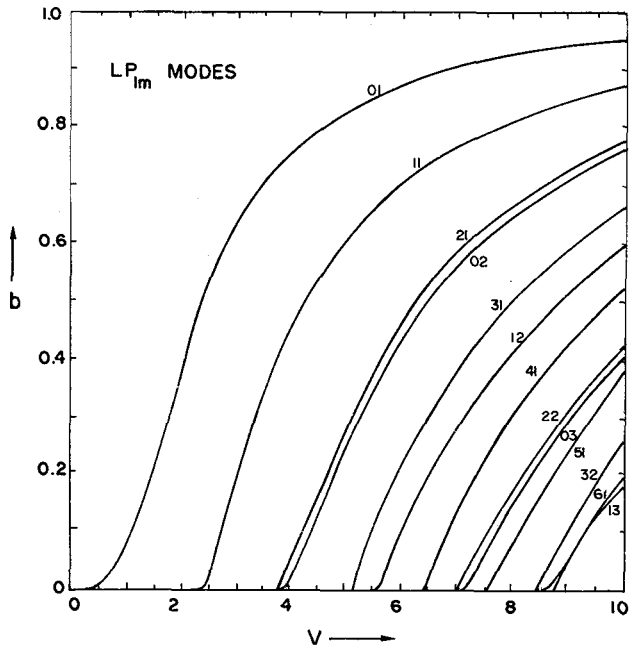


Fig.7 - Normalized propagation parameter  $b=(\beta/k) - n_2/(n_1-n_2)$  as a function of normalized frequency V (See Appendix).

## 4. CONCLUSION

We have observed stimulated Raman scattering (SRS) in various fibers with different characteristics under identical experimental conditions. Although most of our observations can be explained by the theory, our results on pump-to-Stokes power conversion indicate that this effect in fibers is not properly described by existing theoretical models. We suggest that a correct description must take into account the extreme length over which light is kept at very high intensities in optical fibers. Pump power and fiber length have been shown to be equivalent parameters, which could be expected for pump undepleted, but our results extend to the extreme situation of pump extinction. We are presently working on a theoretical model to describe our data.

The authors are thankful for financial support from Telebrás, FAPESP and CNPq (Brazil).

## APPENDIX

This appendix is an extract of Ref. 17. The propagation constant  $\beta$  of any mode of a fiber is limited within the interval  $n_1 > \beta/k > n_2$ , where  $n_1$  is the core and  $n_2$  the cladding refractive indices and  $k = 2\pi/\lambda$  is the wavenumber in free space. We can define two auxiliary parameters

$$u = \alpha(k^2 n_1^2 - \beta^2)^{1/2}$$

$$w = \alpha(\beta^2 - k^2 n_2^2)^{1/2},$$

where  $\alpha$  is the core radius, so that the mode fields can be expressed by Bessel functions of the first kind  $J_\ell(\frac{u r}{\alpha})$  in the core, and of the third kind (Hankel)  $K_\ell(\frac{w r}{\alpha})$  outside the core. The quadratic summation  $V^2 = w^2 + u^2$  gives

$$V = \frac{2\pi\alpha}{\lambda} \sqrt{n_1^2 - n_2^2}$$

which can be considered a *normalized frequency*. The solutions for  $u$  and  $w$  can be obtained (see Ref. 17), and the propagation constant  $\beta$  calculated. Results are depicted in Fig. 7, where not  $\beta$  but

$$b = 1 - \left( \frac{u^2}{V^2} \right) = \frac{(\beta^2/k^2) - n_1^2}{n_1^2 - n_2^2}$$

is plotted in the approximation for  $\Delta \ll 1$ :

$$b \approx \frac{(\beta/k) - n_1}{n_1 - n_2}$$

The number of modes propagating in the core is approximately given by  $N \approx V^2/2$ .

## REFERENCES

1. E.P. Ippen, Appl.Phys.Lett. 16, 303 (1970).
2. R.G.Smith, Appl.Opt. 11, 2489 (1972).
3. G.E.Walrafen, J. Stone, Appl.Spectroscopy 26, 585 (1972).
4. R.H.Stolen, E.P. Ippen, A.R.Tynes, Appl.Phys.Lett. 20, 62 (1972).
5. See, for example (as well as included references): C.Lin, R.H.Stolen, W.French, T.Malone, Opt.Lett., 1, 96 (1977); D.Johnson, K.Hill, B.Kawasaki, D.Kato, Electron.Lett. 13, 53 (1977); C.Lin, B. Marshall, M.Nelson, J.Theobald, Appl. Opt. 17, 2486 (1978); P.Labudde, H.P.Weber, R.H.Stolen, IEEE J. Quantum Electron. QE-16, 115 (1980); C. Lin, L.Cohen, R.H.Stolen, G.W.Tasker, W.French, Opt.Commun. 20, 426(1977); J.Botineau, F.Gires, A.Saissy, C.Vanneste, A.Azema, Appl.Opt.17, 1208 (1978).
6. E.P. Ippen, R.H.Stolen, Appl.Phys.Lett. 21, 539 (1972); K.Hill, D. C. Johnson, B. Kawasaki, Appl. Phys. Lett. 29, 185 (1976).
7. R.H.Stolen, J.E.Bjorkholm, A.Ashkin, Appl. Phys.Lett. 24,308 (1974); K.O.Hill, D.C.Johnson, B.S.Kawasaki, R.Mac Donald, J.Appl.Phys. 49, 5098 (1978).
8. R.W.Hellwarth, IEEE J. Quantum Electron. QE-15, 101 (1979); and references therein.
9. H.R.Stolen, C.Lin, Phys. Rev. A 17, 1448 (1978).

10. R.W.Hellwarth, Phys.Rev. 230, 1850 (1963). R.H.Stolen, E.P. Ippen, Appl.Phys.Lett. 22, 276 (1973).
11. N.Bloembergen, *Nonlinear Optics*, Benjamin, New York (1965).
12. R.H.Stolen, IEEE J.Quantum Electron. QE-11, 100 (1975).
13. Y.R.Shen, N.Bloembergen, Phys.Rev. 137, A 1787 (1964).
14. D.Von der Linde, M.Maier, W.Kaiser, Phys.Rev.178, 11 (1969).
15. J.Auyeung, A.Yariv, IEEE J. Quantum Electron. QE-14, 347 (1978).
16. E. P. Ippen - in *Laser Application to Optics and Spectroscopy*, Jacobs, Scully, Sargent, Scott, Eds., p. 213, Addison-Wesley, Mass(1975).
17. D.Gloge, Appl. Opt. 10, 2252 (1971).
18. F.R.Barbosa e R.Srivastava, Solid State Commun.34, 305 (1980).